The *m*-component spin glass on a Bethe lattice

A. Braun and T. Aspelmeier

Institut für Theoretische Physik, Universität Göttingen, Friedrich-Hund-Platz 1, 37077 Göttingen, Germany
(Received 18 May 2006; revised manuscript received 19 July 2006; published 26 October 2006)

We study the *m*-component vector spin glass in the limit $m \to \infty$ on a Bethe lattice. The cavity method allows for a solution of the model in a self-consistent field approximation and for a perturbative solution of the full problem near the phase transition. The low-temperature phase of the model is analyzed numerically and a generalized Bose-Einstein condensation is found, as in the fully connected model. Scaling relations between four distinct zero-temperature exponents are found.

I. INTRODUCTION

The spin glass with *m*-component spins in the limit of large *m* is an interesting member of the spin glass family for various reasons. First, in the limit $N \to \infty$ it is replica symmetric.[1] This sets it apart from high-dimensional and mean-field spin glasses with Ising, XY, or Heisenberg spins. Second, it is analytically more tractable than, say, Ising systems since the limit $m \to \infty$ allows for some simplifications, and since the replica symmetric theory is much simpler than the theory for broken replica symmetry. Third, it has been shown[2–4] to have an unusual type of phase transition, namely a generalized Bose-Einstein condensation where the spins condense in a high-dimensional subspace in the low-temperature phase. Furthermore, it has been studied in a field-theoretic approach in high dimensions,[5–7] and by computer simulations in low dimensions.[4,8,9] Finally, the complexity, i.e., the number of metastable states, of the *m*-component vector spin glass has been analyzed.[10]

In this work we study the *m*-component spin glass on a Bethe lattice. The Bethe lattice allows for some exact analytical results, using the cavity method[11] for Ising spin glasses, and the influence of the finite connectivity can be analyzed explicitly. Previous work on Ising spin glasses on random graphs and Cayley trees can be found in Refs. 12–14, where the authors developed a replica symmetric solution in terms of the distribution of effective fields and showed its failure. This solution was then extended to the case of the one-step replica symmetry breaking in Ref. 11. The cavity method has also been applied to structural glasses.[15] Furthermore it has been used very successfully in the field of computer science for optimization problems such as *k*-SAT and vertex cover.[16,17] In our work the cavity method has to be extended in a different direction since cavity fields alone are not sufficient to describe the behavior of a *m*-component spin system and terms of quadratic and higher order need to be taken into account. With this modification, we find a phase transition from a paramagnetic to a replica symmetric spin-glass state at a finite temperature.

The generalized Bose-Einstein condensation is also observed on the Bethe lattice. It is characterized by an exponent μ which describes the scaling of the dimensionality n_0 of the ground-state subspace with the number of spins *N*. For the fully connected model $\mu = 2/5$;[2,3] here we find different and connectivity-dependent values. In addition to μ there are a

number of other zero-temperature exponents: an exponent we call *x* describes the scaling of the ground-state energy $e(m, N)$ per spin and component with *m* for $N = \infty$, the scaling of $e(m, N)$ with *N* for $m = \infty$ is characterized by an exponent *y* and finally, ν is the exponent of the singular part of the eigenvalue spectrum of the inverse susceptibility matrix (for $m = N = \infty$). The exponent *y* has also been studied in Refs. 18 and 19 for Ising spin glasses and in Ref. 20 for various models at finite temperature and we will discuss these different results in the end. In this paper we show that these four exponents are not independent but related by scaling laws. As noted in Ref. 4, the order of limits $m \to \infty$ and $N \to \infty$ is important. Physically, taking $N \to \infty$ first makes most sense. Analytically, it is often more useful to take the opposite order, and this is what we will do in this work. Moreover, the generalized Bose-Einstein condensation can only be observed for the order $m \to \infty$ first. The scaling relations show that even though the order of limits is important, it is possible to obtain information from one order of limits about the other.

The paper is organized as follows. In Sec. II we present the details of our model. In Sec. III we extend the cavity method to *m*-component spins, which we need in Sec. IV to study the phase transition. In Sec. V we examine the generalized Bose-Einstein condensation numerically. The results of this are used to check the scaling relations derived in Sec. VI. We conclude in Sec. VII.

II. MODEL

The spin-glass model we analyze in this work consists of *m*-component vector spins $\vec{s}_i$ on a Bethe lattice. The spins have fixed length $|\vec{s}_i|^2 = m$. The Bethe lattice in the context of disordered systems is a random graph with a fixed connectivity for every spin, equal to $k + 1$ in this work. In such a graph consisting of *N* sites, loops are of order logarithm *N*. Therefore the structure of the lattice is locally treelike. We analyze the model in the $m \to \infty$ limit for which the fully connected spin glass is replica symmetric.[1] The same is expected to hold on the Bethe lattice and we will restrict our work to that case. The generic Hamiltonian for the described model is

$$H = -\sum_{i<j} J_{ij} \vec{s}_i \vec{s}_j. \tag{1}$$

Here the exchange interactions J_{ij} are equal to zero if the spins $\vec{s}_i$ and $\vec{s}_j$ are not nearest neighbors on the Bethe lattice.
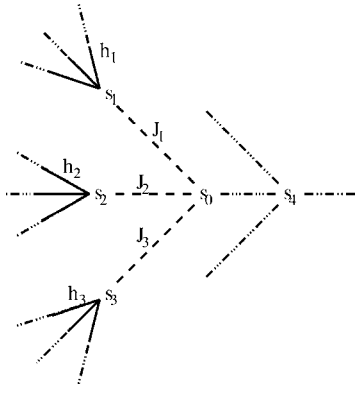
FIG. 1. The three spins $\vec{s}_1$, $\vec{s}_2$, and $\vec{s}_3$ and their back branches are merged onto spin $\vec{s}_0$ with coupling constants J_1, J_2, and J_3 in this example with $k=3$. In the next step of the iteration, $\vec{s}_0$ and two other branches will be merged onto the spin $\vec{s}_4$.

If they are, J_{ij} is drawn from a distribution $P(J_{ij})$ which is either a symmetric bimodal distribution (corresponding to the $\pm J$ model) or a Gaussian distribution. The width of these distributions J' will be chosen to scale with the number of neighbors, such that $J'=J/\sqrt{k}$ with J fixed. This ensures easy comparison in the limit $k\to\infty$ with the fully connected spin glass where $J'=J/\sqrt{N}$.

III. CAVITY METHOD FOR m-COMPONENT SPINS

The cavity method on a $k+1$-connected Bethe lattice for Ising spins is explained in detail in Ref. 11 and we refer the reader to this paper for a review. The main idea for Ising spins is that the local field at a site in the absence of one of its neighbors (the cavity field) is a quantity which can be propagated through the lattice iteratively. This is done by merging k branches of the lattice onto a new spin s_0, see Fig. 1. The many back spins in each branch may be represented by an effective cavity field acting on the end spins s_i. Before merging, the end spins s_i ($i=1,\ldots,k$) of these branches are each missing a neighbor, but after the merger they are $k+1$-connected. The new spin s_0 only has k neighbors from the k branches that are being joined and is thus of the same type as the merged spins $s_1,\ldots,s_k$ were before the merger. The original spins $s_1,\ldots,s_k$ are then traced out, leaving only s_0 with a new effective cavity field (which, of course, depends on the original k cavity fields). This procedure may then be iterated, leading to a recursion relation for the cavity fields which can be used to calculate their distribution $Q(\vec{h})$, see Sec. IV.

In the case of m-component spins this method needs to be modified because a simple vector field is not sufficient to describe the action of k old spins and their effective fields on a new spin. We will see below why this is the case. For the time being, we write the effective Hamiltonian H_i of a k-connected spin i in general form as

$$H_i = -\vec{h}_i\vec{s}_i - \vec{s}_i^{\mathrm{T}}A_i\vec{s}_i - B_i(\vec{s}_i), \tag{2}$$

i.e., a linear term with a field $\vec{h}_i$, a quadratic term with a symmetric traceless matrix A_i, and the rest, contained in the function $B_i(\vec{s})$ which has only terms of order s^3 or higher. The matrix A_i may be chosen to be traceless without loss of generality because any nonzero trace only yields a constant contribution due to the constraint $\vec{s}_i^2=m$. When k such spins are merged onto a new spin s_0 with coupling constants J_i, the partition function of this system is

$$Z_0 = \int \left(\prod_{i=0}^k d^m s_i \delta(m-\vec{s}_i^2) \right) \exp\left\{ -\beta \sum_{i=1}^k (-J_i\vec{s}_0\vec{s}_i + H_i) \right\} \tag{3}$$

$$= \int d^m s_0 \delta(m-\vec{s}_0^2) \prod_{i=1}^k Z_i, \quad \text{where} \tag{4}$$

$$Z_i = \int d^m s_i \delta(m-\vec{s}_i^2) \exp\left\{ -\beta H_i \big|_{\vec{h}_i \to \vec{h}_i+J_i\vec{s}_0} \right\}. \tag{5}$$

Here $\beta=1/k_BT$ is the inverse temperature, as usual. The task is to calculate Z_i and express $\prod_{i=1}^k Z_i$ in the form $\exp\{-\beta H_0\}$ where H_0 has the same functional form as in Eq. (2). We will now proceed in two ways. The first is a self-consistent effective-field approach where we use the description solely in terms of fields, regardless of the fact that it is not sufficient as mentioned above. The effective field will be determined by the condition that it has to reproduce the spin expectation value of the full Hamiltonian. This procedure will show that there is a spin-glass transition at a finite temperature. The second way is to analyze the full problem, which is only possible in the vicinity of the transition. When that is done, it will become clear that near the transition the self-consistent field approach is equivalent to the first-order approximation of the full problem. It may thus be viewed as the first step of a systematic approximation for the whole low-temperature phase.

A. Self-consistent effective-field approach

Setting $A_i=B_i(\vec{s})=0$, we have to calculate

$$Z_i = \int d^m s_i \delta(m-\vec{s}_i^2) \exp\{\beta(\vec{h}_i + J_i\vec{s}_0)\vec{s}_i\}. \tag{6}$$

For notational simplicity, we will abbreviate the term $\vec{h}_i + J_i\vec{s}_0$ by $\tilde{\vec{h}}_i$. We then have

$$Z_i = \int_{-i\infty+c}^{i\infty+c} \frac{dz}{2\pi} \int d^m s_i \exp\{\beta\tilde{\vec{h}}_i\vec{s}_i + z(m-\vec{s}_i^2)\} \tag{7}$$

$$= \int_{-i\infty+c}^{i\infty+c} \frac{dz}{2\pi} \exp\left\{ \beta^2\tilde{\vec{h}}_i^2/4z + zm - \frac{m}{2}\ln\frac{z}{\pi} \right\}. \tag{8}$$

Here we have used an integral representation of the δ-function and c is an arbitrary positive constant to ensure convergence of the Gaussian integrals over the spin components. The remaining integral over z may be evaluated in the limit $m\to\infty$ using the steepest descent methods. Introducing $\tilde{\vec{h}}_i'=\tilde{\vec{h}}_i/\sqrt{m}$ and $\vec{s}_0'=\vec{s}_0/\sqrt{m}$, the exponent in the integral in Eq.

(8) is $m[\beta^2(\tilde{\tilde{h}}'_i)^2/4z + z - \frac{1}{2}\ln z]$, apart from irrelevant constants. The saddle-point equation is therefore

$$\frac{\partial}{\partial z}\left[\beta^2(\tilde{\tilde{h}}'_i)^2/4z + z - \frac{1}{2}\ln z\right] = 1 - \beta^2(\tilde{\tilde{h}}'_i)^2/4z^2 - \frac{1}{2z} = 0. \tag{9}$$

The relevant solution of the saddle-point equation is $z = z_i^0 = \frac{1}{4}[1 + \sqrt{1 + 4\beta^2(\tilde{\tilde{h}}'_i)^2}]$ and we get

$$Z_i = \exp\left\{m\left[\beta^2(\tilde{\tilde{h}}'_i)^2/4z_i^0 + z_i^0 - \frac{1}{2}\ln z_i^0\right]\right\}. \tag{10}$$

Note that according to Eq. (7) this is nothing but the partition function of a single spin in a field $\tilde{\tilde{h}}_i$. Therefore one can obtain the spin expectation value in a field by taking the derivative with respect to $\tilde{\tilde{h}}_i$,

$$\langle \vec{s}_i \rangle = \frac{1}{\beta}\frac{\partial \ln Z_i}{\partial \tilde{\tilde{h}}_i} = \frac{\beta\tilde{\tilde{h}}_i}{2z_i^0} = \frac{2\beta\tilde{\tilde{h}}_i}{1 + \sqrt{1 + 4\beta^2(\tilde{\tilde{h}}'_i)^2}}. \tag{11}$$

We will need this result below.

We can now calculate the propagated partition function Z_0. For that purpose, the term $J_i\vec{s}_0$ that was hidden in $\tilde{\tilde{h}}_i$ must be reintroduced, i.e., we have $z_i^0 = \frac{1}{4}[1 + \sqrt{1 + 4\beta^2(\tilde{h}'_i + J_i\vec{s}'_0)^2}]$ in the following. According to Eqs. (4) and (10), the partition function for spin $\vec{s}_0$ is

$$Z_0 = \int d^m s_0 \delta(m - \vec{s}_0^2)\exp\left\{m\sum_{i=1}^k\left[\beta^2(\vec{h}'_i + J_i\vec{s}'_0)^2/4z_i^0 + z_i^0\right.\right.$$
$$\left.\left. - \frac{1}{2}\ln z_i^0\right]\right\}. \tag{12}$$

Here it can be seen explicitly that Z_0 is not the partition function of a single spin in a field and that the cavity method does not close on the level of fields. The self-consistent approximation now consists of finding a field $\vec{h}_0$ which generates the same spin expectation value as the partition function Z_0. In order to calculate the latter [the former has already been calculated above in Eq. (11)], we again need to employ the steepest descent methods, but this time not only for the auxiliary variable z from the integral representation of the δ-function, but also for all m spin components s_0^α. Here the problem arises that the number of integration variables $m + 1$ is of the same order as the large parameter in the integrand, m. In such a situation the steepest descents cannot be used. The situation is remedied, however, by the following observation. The spin $\vec{s}_0$ only appears in the combination $(\vec{h}_i + J_i\vec{s}_0)^2 = \vec{h}_i^2 + 2J_i\vec{h}_i\vec{s}_0 + mJ_i^2$, so all components of $\vec{s}_0$ orthogonal to the $\vec{h}_i$ are projected out. These $m - k$ orthogonal components may be integrated out first as they are merely Gaussian integrals, leaving only $k + 1$ nontrivial integrals which may then be treated with the saddle-point method. Denoting by O the orthogonal transformation $\vec{t} = O\vec{s}_0$ which transforms the spin variables such that only the integrals over the first k components remain while the rest can be carried out (the details of this transformation are unimportant, as will become apparent below), we get $(\vec{h}_i + J_i\vec{s}_0)^2 = \vec{h}_i^2 + 2J_i(O\vec{h}_i)\vec{t} + mJ_i^2$ and $z_i^0 = \frac{1}{4}\{1 + \sqrt{1 + 4\beta^2[(\vec{h}'_i)^2 + 2J_i(O\vec{h}'_i)\vec{t}' + J_i^2]}\}$ with $\vec{t}' = \vec{t}/\sqrt{m}$. The vector $\vec{t}$ initially has m components, but after carrying out the integrals over the last $m - k$ components, only k components remain and one gets

$$Z_0 = \int_{-i\infty}^{i\infty}\frac{dz}{2\pi}\int d^k t \exp\left(m\sum_{i=1}^k\left\{\beta^2[(\vec{h}'_i)^2 + 2J_i(O\vec{h}'_i)\vec{t}' + J_i^2]/4z_i^0 + z_i^0 - \frac{1}{2}\ln z_i^0 + z[1 - (\vec{t}')^2]\right\} - \frac{m-k}{2}\ln\frac{z}{\pi}\right). \tag{13}$$

The saddle-point equations following from this are

$$z = \frac{1}{2[1 - (\vec{t}')^2]} \tag{14}$$

$$2z\vec{t} = \sum_{i=1}^k\frac{2\beta^2 J_i O\vec{h}_i}{4z_i^0}. \tag{15}$$

Since $\vec{t}$ is merely the transformed spin $\vec{s}_0$, the saddle-point value of $\vec{t}$ immediately gives the expectation value of the spin via $\langle\vec{s}_0\rangle = O^T\vec{t}$ (padding the last $m - k$ components of $\vec{t}$

with zeros). Multiplying Eq. (14) by $2\langle\vec{s}_0\rangle$ yields

$$2z\langle\vec{s}_0\rangle = \frac{\langle\vec{s}_0\rangle}{1 - \langle\vec{s}_0\rangle^2}, \tag{16}$$

while applying O^T from the left to Eq. (15) results in

$$2z\langle\vec{s}_0\rangle = \sum_{i=1}^k\frac{\beta^2 J_i\vec{h}_i}{2z_i^0}. \tag{17}$$

Inside z_i^0, $\vec{t}$ may likewise be replaced by $O\langle\vec{s}_0\rangle$, such that $z_i^0 = \frac{1}{4}\{1 + \sqrt{1 + 4\beta^2[(\vec{h}'_i)^2 + 2J_i\vec{h}'_i\langle\vec{s}'_0\rangle + J_i^2]}\}$.

We are now in a position to present the equation which determines the effective field. It follows from Eq. (11) that, if the spin $\vec{s}_0$ were only subject to a field $\vec{h}_0$, one would have $\beta \vec{h}_0 = \frac{\langle \vec{s}_0 \rangle}{1 - \langle \vec{s}_0 \rangle^2}$. Combining this with Eqs. (16), (17), and again Eq. (11), one gets

$$\vec{h}_0 = \sum_{i=1}^{k} \frac{2\beta J_i \vec{h}_i}{1 + \sqrt{1 + 4\beta^2 [(\vec{h}_i')^2 + 4\beta J_i \dfrac{\vec{h}_i' \vec{h}_0'}{1 + \sqrt{1 + 4\beta^2 (h_0')^2}} + J_i^2]}}, \tag{18}$$

with $\vec{h}_0' = \vec{h}_0 / \sqrt{m}$. This complicated implicit equation determines the field $\vec{h}_0$ which produces the same spin expectation value as Z_0. It corresponds to the Ising analogue $h_0 = \sum_{i=1}^{k} u(J_i, h_i)$ from Ref. 11 where $u(J_i, h_i) = \frac{1}{\beta} \text{atanh}(\tanh \beta J_i \tanh \beta h_i)$. In our context, the presence of $\vec{h}_0$ on the right-hand side of Eq. (18) makes the solution much more difficult. Above and close to the phase transition, however, an expansion of Eq. (18) in powers of $\vec{h}_i$ should be valid. To first order this yields

$$\vec{h}_0 = \sum_{i=1}^{k} \frac{2\beta J_i \vec{h}_i}{1 + \sqrt{1 + 4\beta^2 J_i^2}}. \tag{19}$$

B. Analysis of the full problem

We now turn to the full problem with the Hamiltonian from Eq. (2). As before for the self-consistent effective-field approach, we will denote the term $\vec{h}_i + J_i \vec{s}_0$ by $\tilde{\vec{h}}_i$ in the partition function Z_i. The partition function Z_i may be calculated perturbatively in the following way:

$$Z_i = \int_{-i\infty+c}^{i\infty+c} \frac{dz}{2\pi} \int d^m s_i \exp\{\beta [\tilde{\vec{h}}_i \vec{s}_i + \vec{s}_i^T A_i \vec{s}_i + B_i(\vec{s}_i)] + z(m - \vec{s}_i^2)\} \tag{20}$$

$$= \int_{-i\infty+c}^{i\infty+c} \frac{dz}{2\pi} \int d^m s_i \exp\left\{ \beta \left[\tilde{\vec{h}}_i \vec{s}_i - \vec{s}_i^T \left(\frac{z}{\beta} - A_i \right) \vec{s}_i \right] + mz \right\} \sum_{n=0}^{\infty} \frac{[B_i(\vec{s}_i)]^n}{n!} \tag{21}$$

$$= \int_{-i\infty+c}^{i\infty+c} \frac{dz}{2\pi} \exp\left\{ mz + \frac{\beta}{4} \tilde{\vec{h}}_i^T \left(\frac{z}{\beta} - A_i \right)^{-1} \tilde{\vec{h}}_i - \frac{1}{2} \ln \det \left(\frac{z}{\beta} - A_i \right) + \frac{m}{2} \ln \pi \right\} \sum_{n=0}^{\infty} \frac{\langle B_i^n \rangle_i}{n!} \tag{22}$$

$$= \int_{-i\infty+c}^{i\infty+c} \frac{dz}{2\pi} \exp\left\{ mz + \frac{\beta}{4} \tilde{\vec{h}}_i^T \left(\frac{z}{\beta} - A_i \right)^{-1} \tilde{\vec{h}}_i - \frac{1}{2} \ln \det \left(\frac{z}{\beta} - A_i \right) + \frac{m}{2} \ln \pi \right\} \tag{23}$$

$$\times \exp\left\{ \langle B_i \rangle_i + \frac{1}{2} (\langle B_i^2 \rangle_i - \langle B_i \rangle_i^2) + \cdots \right\}. \tag{24}$$

The angular brackets $\langle \ \rangle_i$ denote the average with respect to the weight $\exp\{\beta[\tilde{\vec{h}}_i \vec{s}_i - \vec{s}_i^T(\frac{z}{\beta} - A_i)\vec{s}_i]\}$. The expression $\frac{z}{\beta} - A_i$ should be interpreted as a matrix expression, i.e., as $\frac{z}{\beta}\mathbb{1} - A_i$. The dots in the last line above indicate higher order cumulants. Now Z_i from Eq. (24) can again be treated by the steepest descent methods in the limit $m \to \infty$, and the resulting saddle-point equation is

$$1 = \frac{1}{4} (\tilde{\vec{h}}_i')^T \left(\frac{z}{\beta} - A_i \right)^{-2} \tilde{\vec{h}}_i' + \frac{1}{2m\beta} \text{Tr}\left(\frac{z}{\beta} - A_i \right)^{-1} - \frac{1}{m} \frac{\partial \langle B_i \rangle_i}{\partial z}$$

$$+ \cdots. \tag{25}$$

The quantity $\langle B_i \rangle_i$ can itself be calculated by steepest descents and is given by $\langle B_i \rangle_i = B_i\left(\frac{1}{2}(\frac{z}{\beta} - A_i)^{-1} \vec{h}_i \right) + \mathcal{O}(1)$. Note that the Hamiltonian Eq. (2) must be extensive in the number of degrees of freedom, which are the m spin components. Therefore the leading term in $\langle B_i \rangle_i$ is of order m. The higher order cumulants can be calculated similarly.

For simplicity, we will only consider the case $B_i(\vec{s}_i) = 0$ and $\vec{h}_i$ and A_i small in the following, which is valid in the vicinity of the phase transition. However, an extension to higher orders is, in principle, straightforward. For small $\vec{h}_i$ and A_i Eq. (25) can be solved perturbatively. For bookkeeping purposes a factor of ϵ will be attached to $\vec{h}_i$ and a factor of ϵ^2 to A_i. It will become clear below that this ansatz is consistent. A perturbative solution of Eq. (25) to second order in ϵ yields

$$Z_i = \exp\left\{ \frac{\beta^2 J_i}{2z_i^{00}} \epsilon \vec{h}_i \vec{s}_0 + \frac{\beta^3 J_i^2}{4(z_i^{00})^2} \epsilon^2 \vec{s}_0^T A_i \vec{s}_0 - \frac{\beta^4 J_i^2}{4m(z_i^{00})^2 \sqrt{1 + 4\beta^2 J_i^2}} \epsilon^2 (\vec{s}_0 \vec{h}_i)^2 + \text{const.} + \mathcal{O}(\epsilon^3) \right\}. \tag{26}$$

Here $z_i^{00} = \frac{1}{4}(1 + \sqrt{1 + 4\beta^2 J_i^2})$ is the limit of z_i^0 as $\vec{h}_i \to 0$. From Eq. (4) Z_0 can be assembled and, setting $\epsilon = 1$, the new $\vec{h}_0$ and A_0 can be read off. They are given by

$$\vec{h}_0 = \sum_{i=1}^{k} \frac{\beta J_i \vec{h}_i}{2z_i^{00}} \tag{27}$$

$$A_0 = \sum_{i=1}^{k} \left(\frac{\beta^2 J_i^2}{4(z_i^{00})^2} A_i - \frac{\beta^3 J_i^2}{4m(z_i^{00})^2 \sqrt{1 + 4\beta^2 J_i^2}} \vec{h}_i \otimes \vec{h}_i \right).$$

(28)

The symbol $\otimes$ denotes the tensor product. Equation (26) shows that the new $\vec{h}_0$ and A_0 are of order ϵ, respectively, ϵ^2 such that the ansatz made above is indeed consistent.

Comparison of Eqs. (19) and (27) shows that the self-consistent effective-field approximation and the solution of the full problem are identical to first order in $\vec{h}_i$.

IV. CALCULATION OF THE PHASE TRANSITION

So far we have described how to iterate on the Bethe lattice with a given realization of the disorder. In order to describe the typical behavior, we need to average over the disorder. For simplicity, we will focus on the self-consistent effective-field approach first.

A. Phase transition at the self-consistent effective-field level

Instead of having a certain cavity field at each site, we now need to find the distribution $Q(\vec{h})$ of cavity fields. Under the assumption that for $m = \infty$ the spin glass is replica symmetric, there is only one such distribution which can be found by solving the functional fixpoint equation

$$Q(\vec{h}) = E_J \int \left(\prod_{i=1}^{k} d^m h_i Q(\vec{h}_i) \right) \delta[\vec{h} - \vec{h}_0(\{J_i\}, \{\vec{h}_i\})], \quad (29)$$

where $\vec{h}_0(\{J_i\}, \{\vec{h}_i\})$ is the solution of Eq. (18). This equation reflects the fact that on average, all sites are identical such that the new distribution of fields on the left-hand side is the same as that of the k-merged spins under the integral on the right-hand side. The symbol E_J stands for the average over the coupling constants J_i. Note that Eq. (29) has the trivial solution $Q(\vec{h}) = \delta(\vec{h})$. In the paramagnetic high-temperature phase the trivial solution is expected to be stable while below the transition temperature it becomes unstable. This will be explicitly verified in the following.

The phase transition takes place when, coming from high temperatures, the true local field becomes nonzero for the first time because it is linked to the Edwards-Anderson order parameter $q_{EA} = \langle \vec{s} \rangle^2$ via Eq. (11). The true local field $\vec{h}_t$ is the field which arises when joining $k+1$ spins at a site, and its distribution is therefore $Q_t(\vec{h}_t) = E_J \int (\prod_{i=1}^{k+1} d^m h_i Q(\vec{h}_i)) \delta[\vec{h}_t - \vec{h}_0(\{J_i\}, \{\vec{h}_i\})]$ where $\vec{h}_0$ is the solution of Eq. (18) but with the sum extending to $k+1$ instead of k. It is thus closely related to the distribution $Q(\vec{h})$ of the cavity fields, and its variance is zero if and only if the variance of $Q(\vec{h})$ is zero.

We analyze the variance of the distribution $Q(\vec{h})$ by regarding Eq. (29) as an iterative prescription. By making a Gaussian ansatz for $Q(\vec{h})$ with width $\epsilon \ll 1$ on the right-hand side, we calculate the width of the resulting distribution on the left-hand side. If the new width ϵ' is smaller than ϵ, the

TABLE I. The system sizes N and the corresponding numbers of samples D.

N	50	70	100	150	200	300	500	1000	3000
D	200	200	150	120	100	80	50	20	6

iteration converges to $\delta(\vec{h})$, if it is larger, the trivial solution is unstable. Using the approximative Eq. (19), which is valid for small $\vec{h}_i$, the new width is

$$\epsilon'^2 = 4\beta^2 \epsilon^2 k \int dJ_1 P(J_1) \frac{J_1^2}{(z_1^{00})^2}.$$

(30)

Equating ϵ and ϵ', the critical temperature can easily be evaluated for the $\pm J$ model and yields

$$T_c = J\left(1 - \frac{1}{k}\right).$$

(31)

In the limit $k \to \infty$, this agrees with the critical temperature of the fully connected model $T_c = J$.[1] For the Gaussian distribution of bonds, the inverse critical temperature is given by the solution of the equation

$$1 = 4\beta^2 \int \frac{dx}{\sqrt{2\pi} J} \frac{x^2 e^{-x^2/2J^2}}{(1 + \sqrt{1 + 4\beta^2 x^2/k})^2}$$

(32)

which also yields $T_c = J$ in the limit $k \to \infty$.

B. Phase transition for the full model

For the full problem, an equation similar to Eq. (29) can be written down for the distribution function of the matrices A. However, while the new field $\vec{h}_0$ depends only on the old fields $\vec{h}_i$, the matrix A_0 not only depends on the old matrices A_i but also on the old fields, see Eq. (28). Therefore, the question is whether the distribution of A becomes nontrivial at a higher temperature than $Q(\vec{h})$. If it did, there would be another phase transition at that temperature but if it didn't, A would be slaved to the $\vec{h}$ and acquire a nonzero variance at
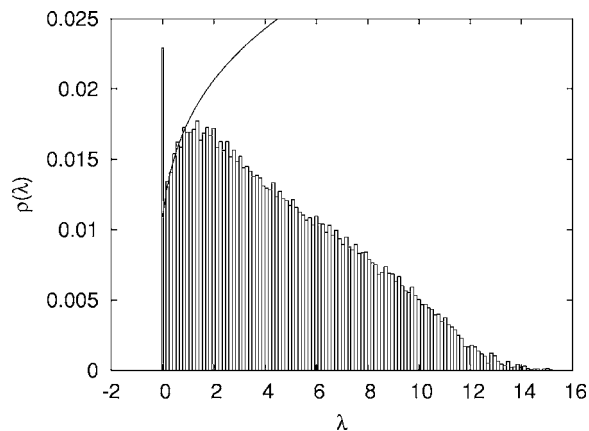

FIG. 2. Eigenvalue density for $N = 300$ and $k+1 = 8$. The dashed line is proportional to $(\Delta\lambda + \lambda)^\nu$ to illustrate that the initial part of $\rho(\lambda)$ scales with the exponent ν.
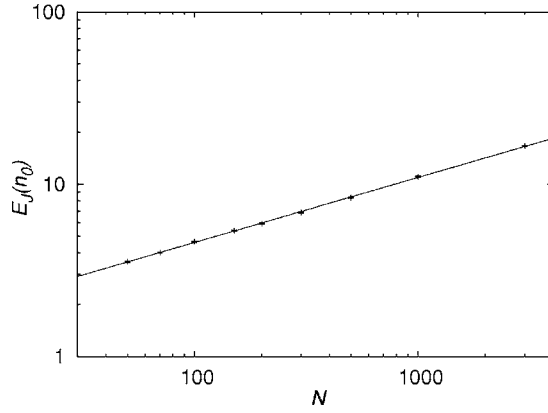
FIG. 3. The number of null eigenvalues for $k+1=8$ as a function of system size N and the fit function $f(N) \sim N^{0.377}$.

the same temperature as $Q(\vec{h})$. Since the calculation is essentially equal to the one shown in the preceding paragraph, we will merely quote the result that the transition temperature of A (in the absence of any fields) for the $\pm J$ model would be $T_c^A = J / \sqrt[4]{k} [1 - (1/\sqrt{k})]$ which is lower than that of the fields for all k, such that there is a common phase transition at temperature T_c. This is, of course, physically sensible and agrees with the results from the fully connected model. The same is expected to hold for all higher orders if the full model is extended to include those orders.

V. GENERALIZED BOSE-EINSTEIN CONDENSATION

So far we have analyzed the phase transition of the model in the thermodynamic limit $N \to \infty$ which is implicit in the cavity method. The generalized Bose-Einstein condensation, which was found for the fully connected model[2,3] and in two-dimensional (2D) and three-dimensional (3D) lattices,[4] can, however, only be detected for finite N. The reason for this is that the dimension n_0 of the ground state is of order N^μ with $0 < \mu < 1$, so the fraction n_0/N vanishes as $N \to \infty$ and the situation becomes indistinguishable from a normal Bose-Einstein condensation for which $n_0=1$. We therefore proceed to analyze the ground state of our model numerically for finite N.

In the ground state every spin is aligned to the direction of its local field,

$$H_i \vec{s}_i = \sum_{j=1}^{N} J_{ij} \vec{s}_j. \tag{33}$$

Here H_i is the modulus of the local field acting on the spin $\vec{s}_i$. This equation can be transformed into the eigenvalue equation $\sum_{j=1}^{N} (H_i \delta_{ij} - J_{ij}) s_j^\alpha = 0$. This eigenvalue equation for the inverse susceptibility matrix $A_{ij} = H_i \delta_{ij} - J_{ij}$ shows that there is at least one null eigenvalue of A. On the other hand, it was shown that A can have at most $\sqrt{2N}$ linearly independent null eigenvectors.[2] Because the dimension of the null eigenspace corresponds to the dimension of the space spanned by the spins,[3] the spins condense into a n_0-dimensional subspace of the m-dimensional space they live in with $0 < n_0 < \sqrt{2N}$. This phenomenon was named generalized Bose-Einstein condensation. The dimension n_0 can be found by iterating Eq. (33) until convergence, and then diagonalizing the matrix A. For the fully connected model it was found that $n_0 \sim N^\mu$ with $\mu = 2/5$.[3]

We have repeated this computation for m-component spins on the Bethe lattice with $k+1=4,6,8$. The accuracy of reaching the ground state was 10^{-7} for the angle between the old and the new direction of every spin $\vec{s}_i$. A list of system sizes and numbers of samples used can be found in Table I. An example for the eigenvalue density of the matrix A and the results for $E_J(n_0)$ are shown in Figs. 2 and 3. Table II shows the results for the exponent μ. The comparison with the results for the fully connected model[3] and for $2d$ and $3d$ models[4] puts the spin glass on the Bethe lattice in between those other models.

VI. SCALING RELATIONS

In Ref. 3 an argument was given to explain the value of $\mu = 2/5$ for the fully connected model model. This value of μ arises as the result of a competition between two energy contributions to the ground-state energy per spin and component $e(m,N) = E/Nm$. The first contribution to e is the ground-state energy as a function of spin components in the limit $N \to \infty$ with m large but fixed. It can be deduced[1,21] that this contribution is $e_0 + \frac{1}{4} m^{-x} + O(m^{-2})$ with $e_0 = -1$ and $x=1$. In the ground state, n_0 plays the role of an effective number of spin components as the spins condense into a n_0-dimensional subspace, thus this contribution is $e_0 + \frac{1}{4} n_0^{-x}$

TABLE II. Results for the exponents μ, ν, x, and y and the ground-state energy per spin and component for different connectivities $k+1$. The exponent x was calculated from μ and ν using Eq. (35); y was calculated from Eq. (37). For comparison, the known values for the fully connected, two- and three-dimensional models are also shown.

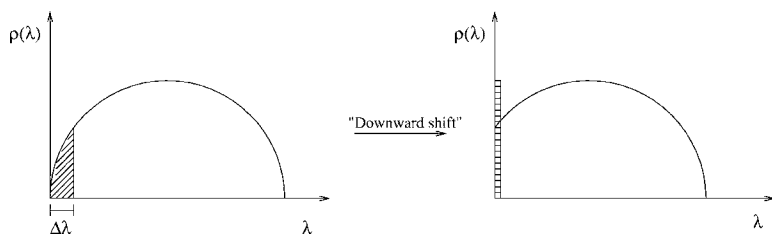| k+1	μ	ν	x	y	e_0
∞	2/5	1/2	1	2/5	−1
8	0.377 (±0.003)	0.234(±0.0003)	1.34(±0.002)	0.505 (±0.004)	−0.83(±0.0016)
6	0.362 (±0.004)	0.217(±0.0003)	1.45(±0.002)	0.525 (±0.006)	−0.80(±0.0015)
4	0.352 (±0.005)	0.168(±0.0013)	1.57(±0.0013)	0.553 (±0.008)	−0.73(±0.0018)
$d=3$[4]	0.33				
$d=2$[4]	0.29				

FIG. 4. The downward shift of the semicircular eigenvalue density of the fully connected *m*-component spin glass: n_0 of the smallest eigenvalues (left, shaded) become null eigenvalues (deltapeak, right)

for $m \geq n_0$. The second contribution consists of additional energy costs resulting from forcing the N spins into a n_0-dimensional subspace. This contribution is important because we are considering the limit $m \rightarrow \infty$ *before* $N \rightarrow \infty$ and n_0 is not fixed but proportional to N^μ. The energy necessary for this can be estimated by the amount the eigenvalue spectrum $\rho(\lambda)$ of A needs to be shifted in order to push n_0 eigenvalues to zero, see Fig. 4. Assuming that the spectrum goes as $\rho(\lambda) \sim \lambda^\nu$ for small λ (such a behavior was predicted for finite dimensional systems[22]), the first n_0 eigenvalues occupy the space from 0 to $\Delta\lambda \sim \left(\frac{n_0}{N}\right)^{1/(\nu+1)}$, so the shift in energy will be of the same order. Combining the two terms we get

$$e = e_0 + c_1 n_0^{-x} + c_2 \left(\frac{n_0}{N}\right)^{1/(\nu+1)} \qquad (34)$$

with two constants c_1 and c_2. Minimizing this relation with respect to n_0 yields the scaling law

$$\mu = \frac{1}{x(\nu+1)+1}. \qquad (35)$$

Inserting the values $x=1$ and $\nu=1/2$ for the fully connected model, we get $\mu=2/5$ as needed. The way we have presented the argument here, however, is more general and applies to the Bethe lattice and finite-dimensional lattices as well.

For the Bethe lattice we do not know the value of x but the scaling relation Eq. (35) may be used to calculate it from μ, which can be measured as described above, and ν, which may be obtained numerically from the eigenvalue spectrum $\rho(\lambda)$. For the latter, it must be kept in mind that we measure the spectra *after* the downward shift, i.e., the spectrum goes

as $\rho(\lambda) \sim (\lambda+\Delta\lambda)^\nu$ (excluding the null eigenvalues), see Fig. 2. The numerical fit was done for $N=3000$ where $\Delta\lambda$ is smallest and we used the integrated eigenvalue density $\Gamma(\lambda)$ which allows for higher precision since there is no need for binning. An example of this fit is shown in Fig. 5 for $k+1 = 8$. The results for the exponent ν are shown in Table II.

In addition to Eq. (35) we can obtain an entirely new scaling relation by making a scaling ansatz for the ground-state energy per spin and component $e(m,N)$ in the following form,

$$e(m,N) - e_0 = m^{-x} F(mN^{-\mu}) \qquad (36)$$

with a scaling function $F(z)$. When we let $N \rightarrow \infty$ while keeping m fixed, this yields $e-e_0 \sim m^{-x}$ as required by the definition of x above [provided $F(0) \neq 0$]. On the other hand, when $m \geq n_0 \sim N^\mu$, we know that the ground-state energy becomes independent of m, so $F(z)=\text{const.} \times z^x$ for $z \geq n_0 N^{-\mu}$ (note that this really is an equality, not just an approximation). From this scaling ansatz it follows that $e(\infty,N)-e_0 \sim N^{-\mu x}$, i.e., the finite-size scaling of the ground-state energy with the number of spin components m taken off to infinity *before* N scales with an exponent

$$y = \mu x = \frac{1-\mu}{1+\nu}. \qquad (37)$$

The second half of this equation stems from eliminating x using Eq. (35). In Fig. 6 we show that this scaling law is, within numerical precision, fulfilled for $k+1=8$. The same goes for the other values of $k+1$ we tested (data not shown). Unfortunately, the data is too noisy to deduce the exponent y
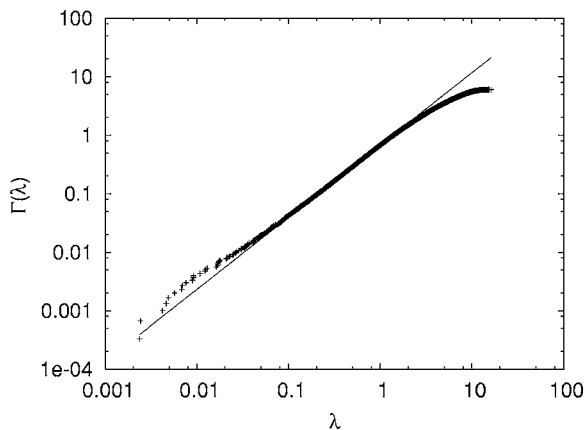

FIG. 5. The integrated eigenvalue density $\Gamma(\lambda)$ for $N=3000$ and $k+1=8$. The straight line has slope $\nu+1=1.234$.
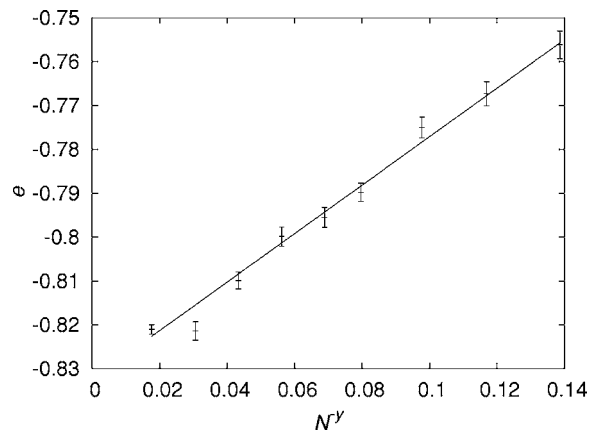

FIG. 6. Ground-state energy per spin and component for $k+1 = 8$ as a function of N^{-y} with y calculated from the scaling relation Eq. (37). The straight line extrapolates to the ground-state energy e_0 in the limit $N \rightarrow \infty$.
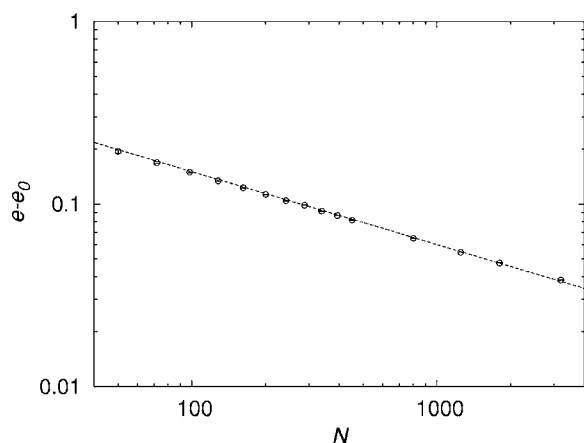
FIG. 7. Ground-state energy per spin and component for the fully connected model. The straight line has slope $-2/5$. The error bars are smaller than the point size.

directly from it. For the fully connected model, Eq. (37) predicts $y=\mu=2/5$. Figure 7 shows that this is indeed observed. In addition to the exponent y, the limiting ground-state energy e_0 can be obtained by extrapolating the data in Fig. 6 to $N=\infty$. The results are listed in Table II. As k increases, e_0 converges towards -1, the value for the fully connected model.

VII. CONCLUSION

In this work we have analyzed the m-component spin glass on the Bethe lattice. By extending the cavity method, we have shown that there is a phase transition from a paramagnetic to a replica symmetric spin-glass state at a finite temperature for all connectivities $k+1>2$. The phase transition is a generalized Bose-Einstein condensation as for the fully connected model.[3] We have examined four different zero-temperature exponents: μ, which describes the scaling of the dimension of the ground state with N (for $m=\infty$); the exponent ν of the singular part of the spectrum of the inverse susceptibility matrix; the exponent x, which determines the scaling of the ground-state energy per spin and component with m (for $N=\infty$); and the scaling exponent y, of the same

quantity with N (for $m=\infty$). These exponents are connected via two scaling laws, Eqs. (35) and (37). As we never used the particular structure of the Bethe lattice in the derivation, we expect the scaling laws to hold in finite dimensions as well. Additionally, the exponents should be the same in the whole low-temperature phase. The exponent ν, for instance, should be the same at finite temperature because it was argued in (Ref. 3) that the eigenvalue spectrum of the inverse susceptibility matrix becomes stuck as soon as the temperature goes below the critical temperature. This is also what happens in the spherical model.[1] At any rate, the scaling laws may be used to obtain the exponent x, which is a quantity of interest because it extrapolates towards finite m for a system in the thermodynamic limit $N=\infty$, from the exponents μ, y, and ν which are defined for $m=\infty$, a case which is often computationally and analytically easier to handle.

Our exponent y is analogous to the shift exponent $1-\Theta_s/d$ as discussed in Ref. 19 for Ising spin glasses. There it was found that $1-\Theta_s/d=2/3$ for all mean-field models considered including the Bethe lattice with connectivities $3,4,6$, and 10. For the fully connected model, this was also confirmed by Billoire.[18] This independence of y of the connectivity is clearly not observed for the $m=\infty$ model, see Table II. For the fully connected model, we found $y=2/5$ and increasing values for smaller connectivities. The origin of this difference in behavior is not clear to us. However, Katzgraber and Campbell[20] have found a similar variation of the exponent with dimensionality for Ising and XY models on hypercubic lattices (our exponent y is analogous to their exponent x/d).

In this work we have presented the leading contribution as $m\rightarrow\infty$. It should be pointed out, however, that our modification of the cavity method can easily be extended to obtain higher order corrections in $1/m$. Work along these lines is in progress.

ACKNOWLEDGMENTS

[1] J. R. L. de Almeida, R. C. Jones, J. M. Kosterlitz, and D. J. Thouless, J. Phys. C **11**, L871 (1978).

[2] M. B. Hastings, J. Stat. Phys. **99**, 171 (2000).

[3] T. Aspelmeier and M. A. Moore, Phys. Rev. Lett. **92**, 077201 (2004).

[4] L. W. Lee, A. Dhar, and A. P. Young, Phys. Rev. E **71**, 036146 (2005).

[5] L. Viana, J. Phys. A **21**, 803 (1988).

[6] J. E. Green, A. J. Bray, and M. A. Moore, J. Phys. A **15**, 2307 (1982).

[7] L. Viana and C. Villarreal, J. Phys. A **26**, 2873 (1993).

[8] B. M. Morris, S. G. Colborne, A. J. Bray, M. A. Moore, and J. Canisius, J. Phys. C **19**, 1157 (1986).

[9] L. W. Lee and A. P. Young, Phys. Rev. E **72**, 036124 (2005).

[10] J. Yeo and M. A. Moore, Phys. Rev. Lett. **93**, 077201 (2004).

[11] M. Mézard and G. Parisi, Eur. Phys. J. B **20**, 217 (2001).

[12] D. R. Bowman and K. Levin, Phys. Rev. B **25**, 3438 (1982).

[13] D. J. Thouless, Phys. Rev. Lett. **56**, 1082 (1986).

[14] M. W. Klein, L. J. Schowalter, and P. Shukla, Phys. Rev. B **19**, 1492 (1979).

[15] O. Rivoire, G. Biroli, O. C. Martin, and M. Mézard, Eur. Phys. J. B **37**, 55 (2004).

[16] A. K. Hartmann and M. Weigt, *Phase Transitions in combinatorial optimization problems: basics, algorithms and statistical*

mechanics (Wiley-VCH, Weinheim, 2005).

[17] A. Braunstein, M. Mézard, and R. Zecchina, Random Struct. Algorithms **27**, 201 (2005).

[18] A. Billoire, Phys. Rev. B **73**, 132201 (2006).

[19] J.-P. Bouchaud, F. Krzakala, and O. C. Martin, Phys. Rev. B **68**, 224404 (2003).

[20] H. G. Katzgraber and I. A. Campbell, Phys. Rev. B **72**, 014462 (2005).

[21] A. J. Bray and M. A. Moore, J. Phys. C **14**, 2629 (1981).

[22] A. J. Bray and M. A. Moore, J. Phys. C **15**, L765 (1982).